

## CONTROL OF AN ELECTROMECHANICAL CAMLESS VALVE ACTUATOR

Chun Tai, Tsu-Chin Tsao<sup>1</sup>

Department of Mechanical and Aerospace Engineering  
University of California at Los Angeles  
Los Angeles, CA 90095

### ABSTRACT

This paper addresses modeling analysis and the soft seating control of an electromagnetic actuator used in electromechanical camless valvetrains. Our mathematical modeling analysis reveals the instability of the actuator dynamics linearized around the seating position and zero velocity. This implies that open loop pulse shaping alone cannot render repeatable valve closing and seating motion. Closed loop feedback control is necessary to generate repeatable motion that is insensitive to disturbances. A linear model is constructed based on gray-box approach that combines mathematical modeling and system identification. Notch filtering and linear quadratic optimal control is designed and experimentally tested. Control performance is evaluated in terms of closing time, valve seating velocity and seating tail-length, armature crossing velocity and armature seating velocity.

### 1. INTRODUCTION

In recent years camless engine has caught much attention in the automotive industry. Camless valvetrain offers programmable valve motion control capability. However, it also introduces valvetrain control issues. There are mainly two types of camless actuators, electrohydraulic valve (EHV) [4][7] and electromechanical valve (EMV) [1][2][3][6][8][9][12] actuators. This paper deals with the EMV type of actuator.

The EMV system discussed in this paper is slightly different from the previous experimental system that the authors had worked on [8][9]. First of all, stronger springs are used in current system setup in order to get faster closing. Secondly, there is no physical lash spring between the engine valve and armature in the new system. The engine valve stem is directly in contact with the armature of the electromagnet. A lash, the clearance between the valve step and the armature when each is seated to its own mechanical stops (valve seat and electromagnet) respectively, of 0.15-0.25 mm is maintained to allow for the valve stem thermal expansion. Thirdly, the position measurement of armature is used for feedback control. The engine valve position is still being monitored, but only for the purpose of modeling and performance evaluation.

For an EMV system, the control of engine valve seating velocity has been identified to be a critical problem. The motion of an engine valve on a conventional engine is driven by a camshaft and constrained by a spring to follow the cam profile. Therefore, small seating velocity is not difficult to achieve. For a camless valvetrain, however, a control system is required to maintain the seating velocity below a given level.

In addition to the results from using the new system and instrumentation described above, in this paper we will present new modeling analyses that shed light to the adequate control system design approach. The objective is to find out what kind of control strategy is suitable for this particular system. Open-loop feedforward control will be the first choice if it is feasible. Cycle-to-cycle iteration upon the open-loop feedforward control could

be considered given the cyclic nature of engine operation and the fact that the system dynamics may change slowly with temperature and aging effect. However, mathematical analysis reveals that an EMV actuator becomes open loop unstable as the engine valve moves close to the seating position. Although stability of the system is not a concern for the finite duration valve closing control problem, instability does indicate large sensitivity and poor repeatability. Therefore open-loop control alone is unlikely to give us acceptable result. Feedback control must be applied for to render consistent soft-seating motion control performance.

### 2. MODELING ANALYSIS

An EMV system consists of two opposing electromagnets, an armature, two springs and an engine valve. The armature moves between the two magnets. When neither magnet is energized, the armature is held at the mid-point of the two magnets by the two springs located on either side of the armature. This system is used to control the motion of the engine valve. The engine valve is then in turn used to control the flow of air into and out of a combustion engine cylinder.

Figure 1 shows the experimental system. Two pulse width modulated (PWM) amplifiers with two DC power supplies are used to drive the two electromagnetic coils of the EMV. Two laser encoder sensors with resolution of 0.6328  $\mu\text{m}$  measure the armature and valve positions. Real-time control program is executed by a Texas Instrument TMS320C32 digital signal processor at 20 KHz sampling rate, implying a velocity resolution of 0.012658 m/sec from the encoder measurement. A PC is used to download program into DSP and upload measured data.

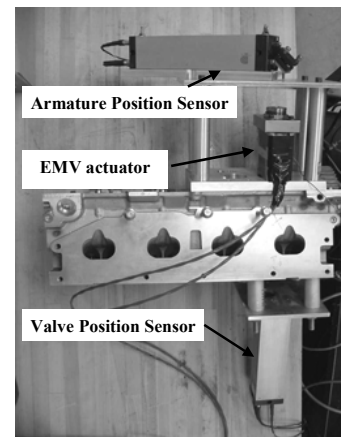


Figure 1. EMV Experimental System

The experimental system discussed in this paper has a natural frequency of 150 Hz, which is higher than the system discussed in the authors' previous papers. Figure 2 shows the free responses of both systems. Neither magnet is energized in these tests when the

<sup>1</sup> Corresponding author's email: [tsao@seas.ucla.edu](mailto:tsao@seas.ucla.edu).

engine valve is released from the fully opened position. Higher natural frequency is necessary for faster valve opening and closing speed in order to operate at high engine speeds.

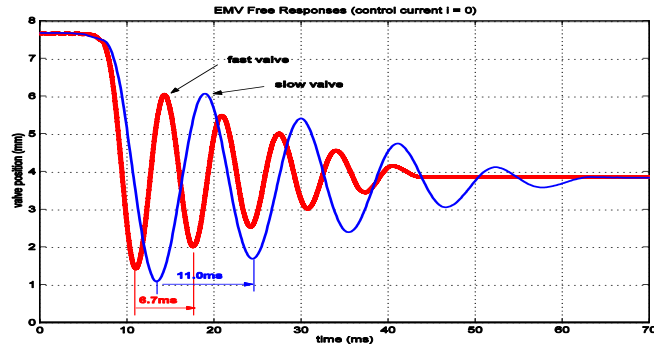


Figure 2. EMV Free Responses with No Current

### 2.1. Power Amplifier

For valve closing, we need to energize the upper solenoid coil shown in Figure 3. It was decided that the power amplifier was set at voltage model instead of current mode, which means that the control variable is the voltage applied on the coil instead of the current. For the upper coil, the voltage and current relationship is governed by the following equation.

$$\frac{L_0}{1 + \frac{x_1}{g}} \frac{di}{dt} = V_s - i \cdot R + \frac{L_0 i}{g \left(1 + \frac{x_1}{g}\right)^2} \frac{dx_1}{dt} \quad (2.1)$$

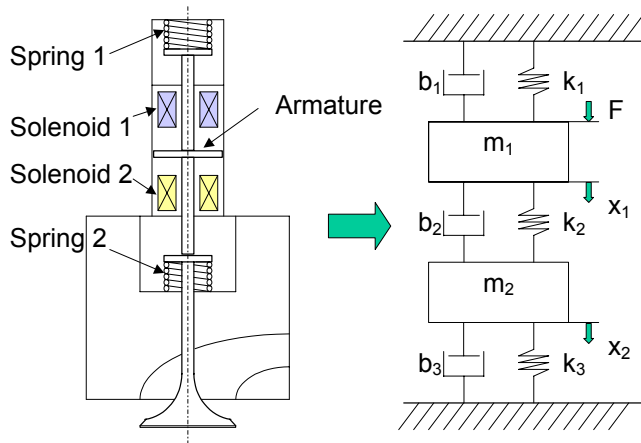


Figure 3. Coordinates for Modeling of EMV Actuator

Previous identification tests show that if the engine valve is fixed at seating position, the step response from voltage to current seems to fit in a first-order prototype, and the time constant is about 3-10 ms. [6] However, when the engine valve is free to move under a certain current, the back-emf effect has to be taken into account. A frequency response from voltage to current is shown in figure 4. No significant phase lag actually appears before 1kHz, and the magnitude variation cross 3 decades is only 20dB. Hence the relationship from voltage to current is modeled as a static gain and the control system design is desired to have at least 20db gain margin.

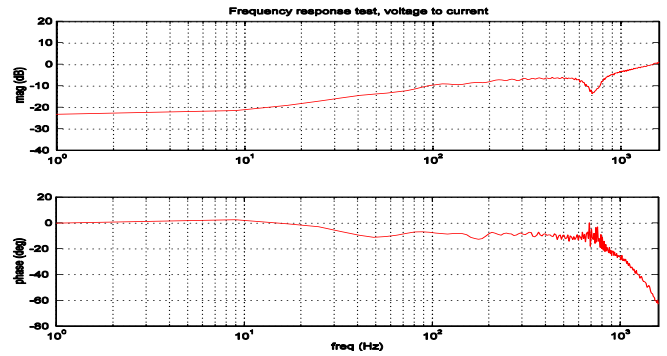


Figure 4. Experimental Frequency Response, voltage to current

### 2.2. Electromagnetic Coils

The current-force relationship is governed by the following equation before magnetic saturation occurs.

$$F = -\frac{L_0 i^2}{2(g + x_1)^2} \quad (2.2)$$

Small signal linearization around some operating position and current gives

$$dF = G_1 \cdot dx_1 + G_2 \cdot di \quad (2.3)$$

where

$$G_1 = \frac{L_0 i^2}{(g + x_1)^3} \quad (2.4)$$

$$G_2 = -\frac{L_0 i}{(g + x_1)^2} \quad (2.5)$$

### 2.3. Spring-Mass System

The mechanical part of the system discussed in this paper is similar as the one discussed in [8] except without having an apparent lash spring. However, it is still necessary to model the connection between the armature and the engine valve as a stiff spring since they are not rigidly connected. The small-signal transfer functions from the current to positions are:

$$\frac{dx_1}{di} = \frac{G_2 \cdot (m_2 s^2 + (b_2 + b_3)s + (k_2 + k_3))}{(m_1 s^2 + (b_1 + b_2)s + (k_1 + k_2 - G_1))(m_2 s^2 + (b_2 + b_3)s + (k_2 + k_3)) - (b_2 s + k_2)^2} \quad (2.6)$$

$$\frac{dx_2}{di} = \frac{G_2 \cdot (b_2 s + k_2)}{(m_1 s^2 + (b_1 + b_2)s + (k_1 + k_2 - G_1))(m_2 s^2 + (b_2 + b_3)s + (k_2 + k_3)) - (b_2 s + k_2)^2} \quad (2.7)$$

Interested readers could refer to the author's previous paper [8] for detailed derivation.

### 2.4. Stability Analysis

As mentioned, a stable system is not necessary for valve closing because an engine valve can be dragged and held on its seating position by large enough electromagnetic in finite time duration. However the sensitivity of the transient motion to disturbances relies much on the system stability. In [8], experimental data of the valve motion under certain open loop control pulse has shown poor repeatability. We may examine the pole locations of the transfer function given in the linearized model in equations (2.3)~(2.6) to analyze the system stability. For stability analysis, we may simplify without loss of generality

the characteristic equation by assuming  $b_1$  and  $b_2$  to be zero. This gives us:

$$(m_1 s^2 + (k_1 + k_2 - G_1))(m_2 s^2 + (k_2 + k_3)) - k_2^2 = 0 \quad (2.8)$$

After reformulating this equation, we have:

$$1 + k_2 \cdot \frac{((m_1 + m_2)s^2 + (k_1 + k_3 - G_1))}{(m_1 s^2 + (k_1 - G_1))(m_2 s^2 + k_3)} = 0 \quad (2.9)$$

$k_2$  is known to be large, therefore the poles of the transfer function are close to  $\sqrt{-\frac{k_1 + k_3 - G_1}{m_1 + m_2}}$ . The system is stable only

if

$$G_1 < (k_1 + k_3) \quad (2.10)$$

Since the electromagnetic force is balanced by the spring force as the valve is held at certain position and the lash spring constant is much greater than the other spring constants, the difference between  $x_1$  and  $x_2$  can be neglected. Therefore the spring force can be expressed as

$$F = (k_1 + k_3)(x_1 - \bar{x}) \quad (2.11)$$

where  $\bar{x}$  is the valve equilibrium position under zero electromagnetic force. The combination of equation (2.2) and (2.11) gives us

$$L_0 \ddot{i}^2 = -2(g + x_1)^2 (k_1 + k_3)(x_1 - \bar{x}) \quad (2.12)$$

Plug equation (2.12) into (2.4), and  $G_1$  can be solved as

$$G_1 = \frac{2(\bar{x} - x_1)}{g + x_1} \cdot (k_1 + k_3) \quad (2.13)$$

To satisfy the stability condition, it is necessary to have

$$\frac{2(\bar{x} - x_1)}{g + x_1} < 1 \quad (2.14)$$

or

$$x_1 > \frac{2\bar{x} - g}{3} \quad (2.15)$$

The air-gap  $g$  can be neglected due to the fact that  $g \ll \bar{x}$  (see [6]). Therefore, the necessary condition for the system to be stable is

$$x_1 > \frac{2}{3}\bar{x} \quad (2.16)$$

Equation (2.16) reveals the instability nature of the electromagnetic type of actuator regardless of the actuator parameters. It tells us that no matter how we choose the spring constants, the valve cannot be held stably at the positions of within one-third of the total lift by open-loop control current. This is important in that neither open-loop control nor cycle-to-cycle iteration only is possible to give us acceptable quiet-seating performance, because the system instability over the one-third point towards the valve seat implies poor repeatability and consistency. Feedback control must be applied to stabilize the system and reduce the sensitivity of the system to disturbance.

The instability of the open-loop control is demonstrated by the following open-loop repeatability test. In this test the control signal is tuned such that the engine valve barely touch the valve seat. Then the tuned control signal is applied to the actuator consecutively for six cycles. The result is shown in Figure 5. Unlike the case of free response when the engine valve consistently settles down at the middle stable equilibrium position, this open-loop feedforward control may or may not close the valve. If we increase the control signal to make sure that the engine valve closes every time, then the seating velocity will be inevitably large.

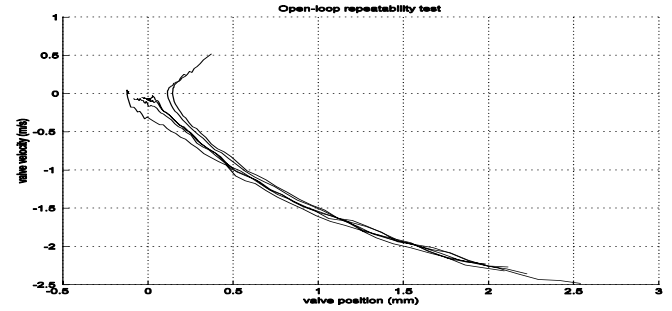


Figure 5. EMV Repeatability Test under Open-loop Control

### 2.5. System Identification

Based on the previous derivation, we parameterize the plant model as following:

$$Gp(s) = \frac{K_2 \left( \frac{s^2}{\omega_3^2} + \frac{2\zeta_3 s}{\omega_3} + 1 \right)}{\left( \frac{s^2}{\omega_1^2} + \frac{2\zeta_1 s}{\omega_1} - 1 \right) \cdot \left( \frac{s^2}{\omega_2^2} + \frac{2\zeta_2 s}{\omega_2} + 1 \right)} \quad (2.17)$$

System identification tests were conducted on the experimental system to extract the unknown parameters in the model. Since the open-loop plant is unstable, the system has to be stabilized with a tuned PD controller before the system identification test could be conducted. Chirp signal was used as the excitation input. The distances of the regulated position to the seating position of these tests are 0.3, 0.5 and 0.7 mm, respectively (Figure 6). Then the parameters of the transfer functions were obtained by curve-fitting the frequency response manually. The difference of the dynamic responses between the armature position and valve position are illustrated in Figure 7. The thin lines are experimental frequency responses, and the thick lines are matching model. The agreement of these frequency responses of different sensor locations validates the model structure we proposed.

### 3. CONTROL DESIGN

When the valve-closing event starts, the lower solenoid coil in Figure 3 is deactivated, and the valve moves up towards its seating position by the mechanical spring force. An EMV actuator works according to the spring-mass pendulum principle, which means that the system follows its own natural oscillation frequency, and external electromagnetic force is only needed for overcoming the friction loss. The electromagnetic actuator is only effective in a relatively short range closing to the seating position, and so it is not efficient in the sense of energy consumption to apply closed-loop control when the valve is still far away from the

seating position. However, previous analysis in section 2.4 shows that the system goes unstable as the engine valve moves to the region within one-third of the total lift. Therefore, the closed-loop control should start at least before this critical point.

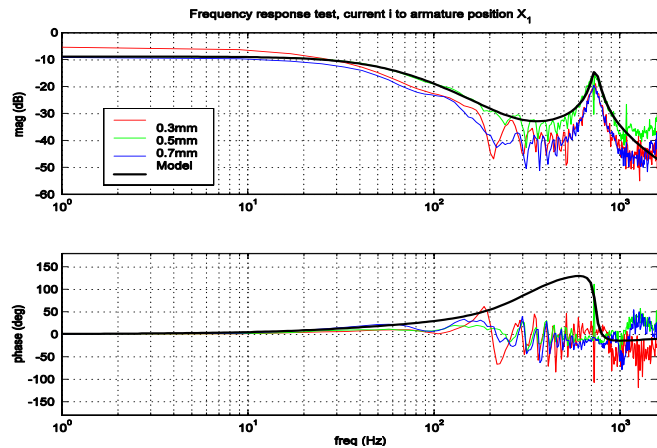


Figure 6. Experimental Frequency Response, Voltage to Armature Position

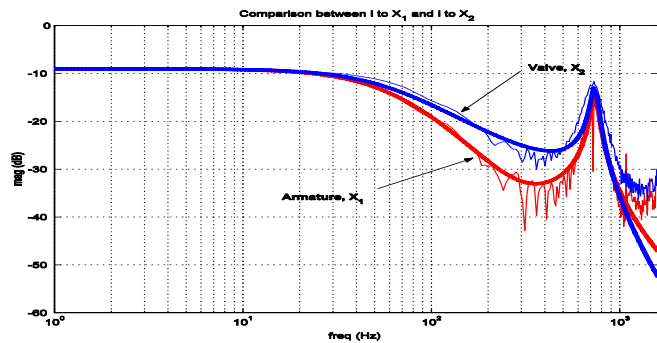


Figure 7. Difference of the Dynamic Responses between the Armature position and Valve Position

The relatively large gain variation shown in the modeling process tells us that the designed control system should have relative large gain margin. Linear-quadratic optimal control design is chosen for this purpose.

The control structure is shown in Figure 8.  $G_p$  is the plant model.  $G_n$  is a notch filter, which will be explained in section 3.1.  $G_c$  is a stabilizing controller, which will be designed in section 3.2. The feedforward signal  $u_{ff}$  will be discussed in section 3.3.

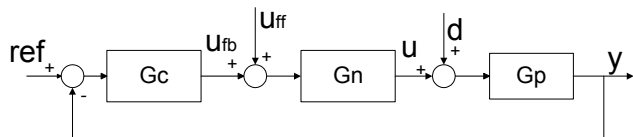


Figure 8. Control Structure

### 3.1. Notch filter

The plant has been identified to be fourth order model. It is noticed that the lightly-damped second-order pole-zero pair should be canceled out before the optimal control design is applied.

$$G_n(s) = \frac{s^2 + \frac{2\zeta_2 s}{\omega_2} + 1}{\frac{s^2}{\bar{\omega}_2^2} + \frac{2\zeta_3 s}{\omega_3} + 1} \quad (3.1)$$

Ideally,  $\bar{\omega}_2$  should be equal to the resonant model  $\omega_2$  for perfect cancellation. However, in real implementation,  $\bar{\omega}_2$  should be set to be a little bit smaller than  $\omega_2$  for the robustness of design. The necessity of having this notch filter has been demonstrated by experiments in the authors' previous paper. [9]

### 3.2. LQ Optimal Control Design

The augmented plant, i.e. the plant cascaded with the notch filter, is converted into state-space form.

$$\dot{x}(t) = Ax(t) + Bu(t) \quad (3.2)$$

$$y(t) = Cx(t) \quad (3.3)$$

This model has two states, the armature position and velocity. The position can be directly measured, and the velocity can be estimated with the differentiation of position measurements. An LQ optimal controller is designed for stabilizing the augmented plant. The cost function that needs to be minimized is

$$J = \int_0^{\infty} (x^T(t)Qx(t) + Ru^2(t)) \cdot dt \quad (3.4)$$

where  $Q$  and  $R$  need to be chosen based on the given system. The final control law is given by

$$u(t) = -R^{-1}B^T Px(t) \quad (3.5)$$

where  $P$  is the solution to the Riccati algebraic equation

$$A^T P + PA - PBR^{-1}B^T P + Q = 0 \quad (3.6)$$

### 3.3. Feedforward Control Sequence and Trajectory Design

A natural way to control the valve seating process is that we first tune an open-loop control signal sequence such that the provided energy barely matches the friction loss. By applying this control sequence, sometimes the valve close with very small seating velocity, but sometimes it does not close at all due to the instability nature of the system. Now we pick the case when the valve lands smoothly with acceptable seating velocity, record the armature motion trajectory and use it as the reference trajectory for the closed-loop system to track. Meanwhile the tuned open-loop control signal sequence serves as the feedforward control signal. The objective of the feedback controller is to reduce the sensitivity of the system to disturbance and maintain valve motion along the given reference trajectory.

## 4. EXPERIMENTAL RESULTS

The design process in section 3 is conducted in continuous-time domain. When it comes to digital implementation, bilinear transformation is used to digitalize the designed controller. The sampling frequency is 20kHz. Since the frequency range of interest is less than 2kHz, the frequency warping effect during the transformation process is neglected.

#### 4.1. Performance Indices

The closing and seating performance of the closed-loop controlled EMV system can be quantified by using the following three indices: Closing Time  $t_c$ , Seating Tail-Length  $t_s$ , Valve Seating Velocity  $v_s$ , Armature Crossing Velocity  $v_c$  and Armature Seating Velocity  $v_a$ .

**Definition 1, Closing Time,  $t_c$ :** The time it takes for the valve to move from 90% of the maximum lift to 10% of the maximum lift.

**Definition 2, Seating Tail-Length,  $t_s$ :** Run a free-response test for the EMV system and record the moment that the engine valve reaches the lowest position (closest to its seat) as time  $t_0$ . Then for each quieting-seating control test, record the moment of the first time the engine valve gets to the seating position as  $t_f$ . The "seating tail-length" is defined as  $t_f - t_0$ .

**Definition 3, Valve Seating Velocity,  $v_s$ :** The instant velocity of engine valve at the first time it gets to its seating position.

**Definition 4, Armature Crossing Velocity,  $v_c$ :** The average velocity of the armature moving from 0.05 mm above the valve seating position to 0.05 mm below the valve seating position.

**Definition 5, Armature Seating Velocity,  $v_a$ :** The instant velocity of armature at the first time it gets to its own mechanical boundary.

The method of finding the seating position in experiments is described in the authors' previous paper [9]. The reason why we have different indices for the valve seating velocity and armature crossing velocity is due to the fact that the armature and valve are not rigidly connected, and their velocities are not necessarily the same. The difference between the armature motion and valve motion is illustrated in Figure 9.

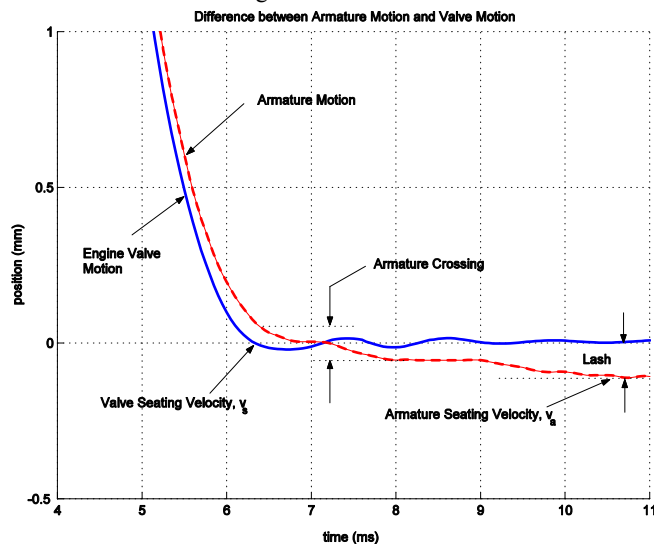


Figure 9. The Difference between Armature Motion and Valve Motion

#### 4.2. Closed-Loop Repeatability Test

In this test we implemented the controller designed in Section 3 to the EMV system, and conducted 50 sweeps of engine cycles. It does not mean much by just having one good (quiet) response because the essential problem we had at the beginning was that the system was sensitive to unknown disturbance. (Indeed, even open-loop control could occasionally render us quiet-seating performance.) Therefore when we test our closed-

loop control system, the most important issue is to see if we can have good and consistent system responses. The 50 sweeps of engine valve motion trajectories are shown in Figure 10.

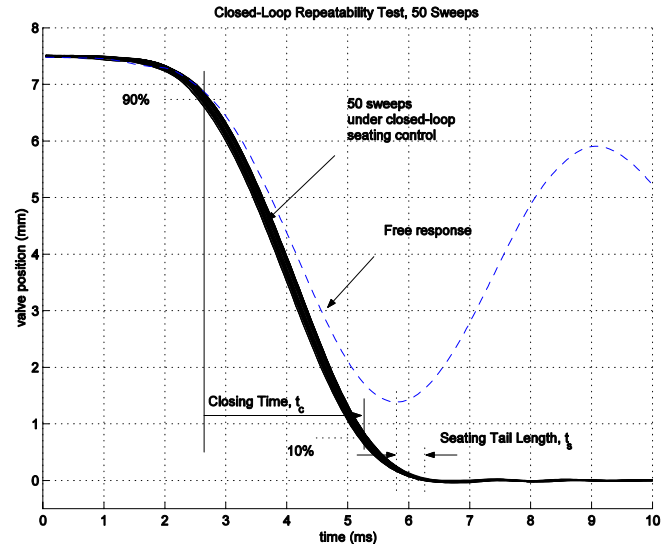


Figure 10. Closed-Loop Repeatability Test

Figure 11 shows the distribution of Valve Seating Velocity,  $v_s$ . Figure 12 shows the distribution of Armature Seating Velocity,  $v_a$ . The mean values and standard deviations for all the performance indices are summarized in Table 1.

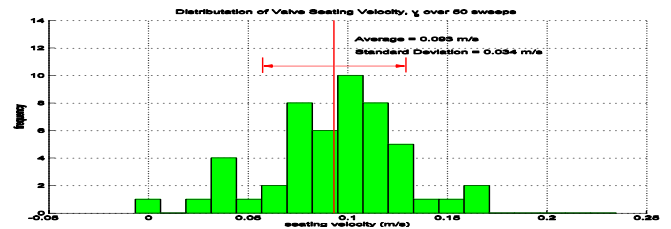


Figure 11. Distribution of Valve Seating Velocity,  $v_s$ , over 50 Sweeps

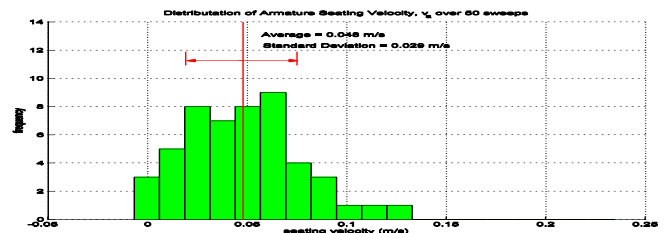


Figure 12. Distribution of Armature Seating Velocity,  $v_a$ , over 50 Sweeps

Table 1. Summary of Closed-Loop Seating Control Result

	Mean	Standard Deviation
Closing Time, $t_c$ , (ms)	2.76	0.02
Seating Tail-Length, $t_s$ , (ms)	0.68	0.30
Valve Seating Velocity, $v_s$ , (m/s)	0.093	0.034
Armature Crossing Velocity, $v_c$ , (m/s)	0.093	0.015
Armature Seating Velocity, $v_a$ , (m/s)	0.048	0.029

### 4.3. Compromise of Supply Voltage and Power Consumption

The supply voltage has to be higher than some minimum required value,  $V_{min}$ , in order for providing enough energy to overcome the system's friction loss. As the supply voltage is higher than  $V_{min}$ , soft-seating may be realized, but depending on how close the supply voltage is to  $V_{min}$ , the power consumption might be high. As we discussed at the beginning of section 3, the electromagnetic actuator is only effective in a relatively short range. Therefore, the energy-efficient way to control the valve is that there is zero current when the valve is far away from the seating position, and high enough current when the valve is close. However, it takes time for the current to build up to the level that is necessary for the valve closing due to the existence of coil inductance, and the time for building up the required current depends on the given supply voltage. Basically, the higher the supply voltage is, the shorter time it takes for the current to build up, and the less energy is wasted during the current transient time.

Seating control was tested with two different supply voltages, 50V and 80V respectively, to demonstrate the trade-off between supply voltage and power consumption. Figure 13 shows the voltage, current and valve motion in both cases. Table 2 lists the energy consumed during the valve closing process in both case. The case with higher supply voltage consumes less energy.

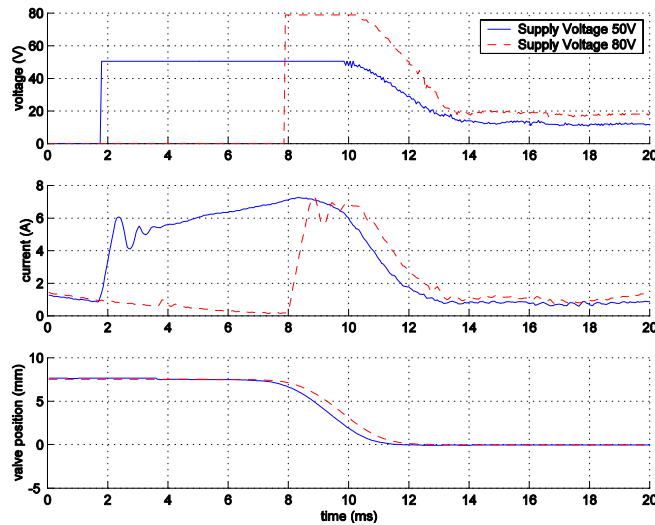


Figure 13. Trade-off between Supply Voltage and Power Consumption

Table 2. Energy Consumption during Valve Closing

Supply Voltage (V)	50	80
Energy Consumption (J)	2.9	1.9

### CONCLUSIONS

Our mathematical modeling analysis reveals that a camless electromechanical valve actuator becomes unstable, as the distance of the engine valve to its seating position is less than roughly one third of the total lift, regardless of spring rate or electromagnetic coil turns. A linear model was obtained based on the derived model structure and system identification test result for control system design. An LQ optimal control is designed and implemented on the hardware system. The experimental results have shown consistent closed-loop system response. The average valve seating velocity is 0.093 m/s with standard deviation of 0.034 m/s and the armature average seating velocity is 0.048 m/s with standard deviation of 0.029 m/s. The closing time is 2.76ms

and seating tail-length is 0.68 ms. Both of them indicate improvement from the authors' previous work with weaker mechanical springs. The compromising relationship between supply voltage and power consumption is discussed and demonstrated by experiments. Present and future research effort is directed toward further improving the valve motion control performance and energy consumption under supply voltage constraint.

### ACKNOWLEDGMENT

The authors gratefully thank Ford Research Lab for lending the electromagnetic actuator and Visteon for providing the mechanical springs used in this work.

### REFERENCES

- [1] Butzmann, S., Melbert, J., and Koch, A., "Sensorless Control of Electromagnetic Actuators for Variable Valve Train," SAE Paper 2000-01-1225
- [2] Hoffmann, W., and Stefanopoulou, A., "Valve Position Tracking for Soft Land of Electromechanical Camless Valvetrain," 3<sup>rd</sup> IFAC Conference Advances in Automotive Control, 2001
- [3] Hoffmann, W., and Stefanopoulou, A., "Iterative Learning Control of Electromechanical Camless Valve Actuator," Proceedings of the American Control Conference, Arlington, VA, June 2001
- [4] Schechter, M., and Levin, M., "Camless Engine," SAE Paper 960581, 1996.
- [5] Skogestad, S. and Postlethwaite, I., Multivariable Feedback Control Analysis and Design, Hohn Wiley & Sons, 1996
- [6] Stubbs, A., "Modeling And Controller Design Of An Electromagnetic Engine Valve," M.S. Thesis, University of Illinois at Urbana-Champaign, 2000
- [7] Tai, C., Tsao, T-C. and Levin, M., "Nonlinear Adaptive Feedforward Control of an Electrohydraulic Camless Valvetrain," *Proc. American Control Conference*, 1001-1005, Chicago, IL, June 2000.
- [8] Tai, C., Stubbs, A. and Tsao, T-C., "Modeling and Controller Design of an Electromagnetic Engine Valve," *Proc. American Control Conference*, 2890-2895, Arlington, VA, June 2001
- [9] Tai, C. and Tsao, T-C., "Quiet Seating Control Design of an Electromagnetic Engine Valve Actuator," *ASME International Mechanical Engineering Congress and Exposition*, New York, NY, November 11-16, 2001.
- [10] Tomizuka, M., Tsao, T-C., and Chew, K-K., "Analysis and Synthesis of Discrete-Time Repetitive Controllers," *Journal of Dynamic Systems, Measurement, and Control*, 1989
- [11] Tsao, T-C., and Tomizuka, M., "Robust Adaptive and Repetitive Digital Tracking Control and Application to a Hydraulic Servo for Noncircular Machining," *Transactions of ASME*, 1994
- [12] Wang, Y., Stefanopoulou, A., Haghgoie, M., Kolmanovsky, I., and Hammoud, M. "Modelling of an Electromechanical Valve Actuator for a Camless Engine," 5th International Symposium on Advanced Vehicle Control, Ann Arbor, Michigan USA, 2000